Acıbadem Univ. Sağlık Bilim. Derg. 2023; 14 (1): 10-23
https://doi.org/10.31067/acusaglik.1210129

In Silico Studies and *In Vitro* Microsomal Metabolism of Potent Metap2 Inhibitor And *In Vivo* Tumor Suppressor for Prostate Cancer: A Thioether-Triazole Hybrid

Göknil Pelin Coşkun[1], Kaan Birgül[2], Asaf Evrim Evren[3,4], Ş. Güniz Küçükgüzel[5], Mert Ülgen[1]

[1]Department of Pharmaceutical Chemistry, Faculty of Pharmacy, Acibadem Mehmet Ali Aydınlar University, Istanbul, Turkey

[2]Department of Pharmaceutical Chemistry, Faculty of Pharmacy, Bahçeşehir University, Beşiktaş, Istanbul, Turkey

[3]Department of Pharmaceutical Chemistry, Faculty of Pharmacy, Anadolu University, Eskişehir, Turkey

[4]Department of Pharmacy Services, Vocational School of Health Services, Bilecik Şeyh Edebali University, 11230 Bilecik, Turkey

[5]Department of Pharmaceutical Chemistry, Faculty of Pharmacy, Fenerbahçe University, Ataşehir, Istanbul, Turkey

Göknil Pelin COŞKUN
Kaan BİRGÜL
Asaf Evrim EVREN
Ş. Güniz KÜÇÜKGÜZEL
Mert ÜLGEN

Correspondence: Göknil Pelin Coşkun
Department of Pharmaceutical Chemistry, Faculty of Pharmacy, Acibadem Mehmet Ali Aydınlar University, Istanbul, Turkey
Phone: -
E-mail: goknilpelincoskun@gmail.com

Received: 25 November 2022
Accepted: 12 December 2022

ABSTRACT

Background/aim: The *in vitro* microsomal metabolism of (*S*)-3-((2,4,6-trimethylphenyl)thio)-4-(4-fluorophenyl)-5-(1-(6-methoxynaphtalene-2-yl)ethyl)-4*H*-1,2,4-triazole (SGK636), an anticancer drug candidate was studied using pig microsomal preparations fortified with NADPH to identify the potential *S*-oxidation and *S*-dealkylation metabolites.

Materials and methods: In the present study, the sulfoxide metabolite was synthesized, purified and characterized by chromatographic and spectroscopic methods. SGK636, the *S*-oxidation and *S*-dealkylation metabolites were then separated by a reversed phase LC-MS, with UV detection and with an HP-TLC system. The results from the in-vitro microsomal metabolic experiments showed that SGK636 produced the corresponding *S*-oxidation metabolite (sulfoxide) which was observed by LC-MS, LC-MS/MS and HP-TLC with the identical Rt and Rfx100 values and UV/MS spectra in comparison with the authentic compounds, but no any *S*-dealkylation metabolite was detected.

Results: The present results were proved with molecular docking and molecular dynamic studies. Since sulfoxidation process can be reversible and it may partly explain the low amount of sulfoxide metabolite in our experiment, we also incubated the sulfoxide. No conversion back to the substrate (SGK636) was observed, but it produced the corresponding sulphone metabolite. In order to establish if SGK636 is autooxidized, the substrate was also incubated in buffer under standard incubation conditions, but no any autooxidation was observed into the corresponding sulfoxide. We also did a stability work for SGK636-SO (sulfoxide) in buffer to see any possible autooxidation to sulfone or reduction back to SGK636. No conversion was observed in either way. The substrate seems to be stable to metabolic reactions and to autooxidation which could be an advantage in terms of its pharmacological activity.

Conclusion: The present metabolic study indicates that SGK 636 underwent *S*-oxidation. In order to identify the responsible oxidative enzyme, molecular docking and molecular dynamic studies were performed. CYP3A4 was found to be responsible enzyme for *S*-oxidation.

Keywords: *S*-oxidation, *in vitro* metabolism, thioether, 1,2,4-triazole, Naproxen

Bir Tiyoeter-Triazol Hibriti: Güçlü MetAP2 Inhibitörü ve Prostat Kanseri için *In Vivo* Tümör Baskılayıcı Bileşiğin *In Silico* Çalışmaları ve *In Vitro* Mikrozomal Metabolizması

ÖZET

Arka plan/amaç: Antikanser bir ilaç adayı bileşik olan (*S*)-3-((2,4,6-trimetilfenil)tiyo)-4-(4-florofenil)-5-(1-(6-metoksinaftalen-2-)il) etil)-4*H*-1,2,4-triazol (SGK636), bileşiğinin in vitro mikrozomal metabolizması çalışılmış ve potansiyel *S*-oksidasyon ve *S*-dealkilasyon metabolitlerini belirlemek için NADPH ile güçlendirilmiş domuz mikrozomal preparatları kullanılarak incelenmiştir.

Gereç ve Yöntemler: Bu çalışmada, sülfoksit metaboliti kromatografik ve spektroskopik yöntemlerle sentezlenmiş, saflaştırılmış ve karakterize edilmiştir. SGK636, *S*-oksidasyon ve *S*-dealkilasyon metabolitleri daha sonra ters fazlı bir LC-MS, UV spektroskopisi ve bir HP-TLC sistemi ile ayrılmıştır. *In vitro* mikrozomal metabolik deneylerin sonuçları, SGK636'nın, aynı Rt ve Rfx100 değerleri ve UV/ ile LC-MS, LC-MS/MS ve HP-TLC tarafından gözlemlenen karşılık gelen *S*-oksidasyon metabolitini (sülfoksit) ürettiğini göstermiştir. Otantik bileşiklerle karşılaştırıldığında MS spektrumlarında, herhangi bir *S*-dealkilasyon metaboliti tespit edilmemiştir.

Bulgular: Mevcut sonuçlar moleküler doking ve moleküler dinamik çalışmalarla kanıtlanmıştır. Sülfoksidasyon işlemi tersine çevrilebilir olduğundan ve deneyimizdeki düşük miktarda sülfoksit metabolitini kısmen açıklayabildiğinden, sülfoksit bileşiği de inkübe edilmiştir. Substrata (SGK636) geri dönüşüm gözlenmemiş olup, karşılık gelen sülfon metabolitinin oluştuğu gözlenmiştir. SGK636'nın otooksidize olup olmadığını belirlemek için substrat ayrıca standart inkübasyon koşulları altında tampon içinde inkübe edilmiştir, ancak karşılık gelen sülfoksitte herhangi bir oto-oksidasyon gözlenmemiştir. Sülfona herhangi bir olası otooksidasyonu veya tekrar SGK636'ya indirgemeyi görmek için tampondaki SGK636-SO (sülfoksit) için bir stabilite çalışması da yapılmıştır. Her iki şekilde de dönüşüm gözlemlenmemiştir. Substrat, farmakolojik aktivitesi açısından bir avantaj olabilecek metabolik reaksiyonlara ve otooksidasyona karşı kararlı görünmektedir.

Sonuç: Mevcut metabolik çalışma, SGK 636'nın *S*-oksidasyonuna uğradığını göstermektedir. Sorumlu oksidatif enzimi belirlemek için moleküler yerleştirme ve moleküler dinamik çalışmalar yapılmıştır. CYP3A4'ün *S*-oksidasyonundan sorumlu enzim olduğu bulunmuştur.

Anahtar kelimeler: S-oksidasyon, *in vitro* metabolizma, tiyoeter, 1,2,4-triazol, Naproksen.

Sulphur containing molecules provide a wide range of place in medicinal chemistry. Many drug molecules carry sulphur atom and some of them show their pharmacological activities depending of sulphur structure. One of the most commonly known drugs in this area are organophosphates. As they show their activity by acetylation of acetyl co-esterases, the metabolic inactivation of these compounds mostly depends on *S*-oxidation or desulphuration (1). Thioethers (or sulfides) can be included in a variety of drugs and potential drug candidates are designed with this group as an isostere of ethers. Phase I reactions are *S*-oxygenation to sulfoxide and sulfones and *S*-dealkylation although the latter is a minor metabolic dealkylation reaction compared to the *N*- or *O*-analogues. Sulfoxide reduction back to the parent sulfide is also possible. The conversion of sulfide to sulfoxide is important in terms of potential pharmacological and toxicological changes in activity (2). Chlorpromazine sulfoxidation is catalyzed by P450 dependent monooxygenases whereas *S*-oxygenation of H2 receptor blockers cimetidine, albendazole, ranitidine, and sulindac is catayzed by flavin containing monooxygenases (3). Sulfoxidation is reported as minor metabolic pathway for the urinary rat metabolism of H2 receptor blockers cimetidine, ranitidine and nizatidine (4). Earlier studies on sulphur containing compounds were performed by using computational studies with density functional theory. The metabolic profile of dimethylsulfoxide (DMSO) and dimethylsulfide (DMS) was recorded accordingly. As the ability of oxidation and dealkylation reactions high in cytochrome P450 enzyme family, it many times depends on the compound's certain functional groups. The computitonal studies identify the most favorable reaction pathway in sulphur carrying model molecules. It was also observed that *S*-oxidation is more preferred than *S*-dealkylation by the experimental and computational studies on DMSO and DMS (5). Another study showed the metabolic profile of a sulindac derivative in different species both in mouse and human. It was observed that phospho-sulindac amide undergoes hydroxylation reaction to form di-hydroxyl-phospho-sulindac amide and mono-hydroxyl-phospho-sulindac amide. Further investigations with mouse and human liver microsomes showed that phospho-sulindac amide is oxidized or reduced. The oxidation and reduction reactions were observed with the formation of sulfone and sulfide derivatives of phospho-sulindac amide respectively (6). The metabolic pathway from sulfoxide to sulphide has been used on a common non-steroidal anti-inflammatory pro-drug, Sulindac. Sulindac has no cyclooxygenase I (COX-1) or cyclooxygenase II (COX-2) inhibitory activity. However, it undergoes a reversible reduction reaction via biotransformation. The active form of this drug is a thioether derivative (sulindac sulfide). Sulindac also undergoes *S*-oxidation resulting with the formation of a sulfone metabolite which has also no inhibitory activity against COX-1 and COX-2 isoenzymes (7). Limited studies are available related to thioether metabolism in the literature. In these studies, the enzymatic profile of sulphur containing compounds were mentioned. As cytochrome P450 enzyme family plays a vital role in human and animal metabolism, some studies hold flavin monooxyganase responsible for sulfoxide formation. Li and co-workers reported that Compound I (Cpd I) from iron–oxo porphyrin species is responsible for sulfoxide formation (8).

The synthesis and anticancer profile of some thioether containing drug candidate molecules were studied in our previous experiments. As prostate cancer is the second highest incidence of cancer among men, our previous study focused on (*S*)-Naproxen ((+) (*S*)-2-(6-methoxynapthalene-2-yl)propanoic acid) derivatives. It is an active substance that has been reported to have anticancer activities in recent years (9-13). In addition, researchers have reported anticancer activities of Naproxen derivatives in prostate and breast cancer (14-20). On the other hand, many studies have been conducted on compounds containing thioether structures, have anticonvulsant, antidepressant, antimalarial, antiviral, vasodilator, antimicrobial, antiurease and antitumoral activities (19, 21-33). In the light of this information, Birgül and co-workers studied the thioether derivative of Naproxen (16). SGK636 exhibited the best anticancer activity among the tested molecules. The compound showed no toxic profile on the healthy cells, it was found to be valuable to undergo further research in terms of metabolic profile. Our previous work indicated the *in vitro* metabolic profile of some active molecules (34-36). In-vitro and in-vivo metabolic studies are needed to identify the potential metabolites of thioether structures with potential pharmacological activity. In the present work, we therefore planned to study SGK636's in-vitro hepatic microsomal metabolism to observe if it is converted to any *S*-oxidation or dealkylated metabolites. We have performed the synthesis of authentic *S*-oxide metabolic standard of compound SGK636 and elucidated its structure by using spectroscopic methods. This paper also presents for the first time a rapid and simple method for the determination of metabolites using HP-TLC.

MATERIALS AND METHODS

SGK636 and authentic triazole metabolic standard (DT) were previously prepared (16). In the present study, SGK636-SO was synthesized as described later in the text. *m*-Chloroperoxybenzoic acid (*m*-CPBA) and all other chemicals were purchased from Sigma Aldrich and Merck. Melting point was recorded on a Stuart SMP50 Automatic Melting Point apparatus and uncorrected. The structure of SGK636-SO were confirmed by FT-IR, LC-MS, LC-MS/MS spectra and elemental analysis. FT-IR analysis were performed with Thermo Scientific Nicolet IS10 device. LC-MS separation of SGK636, DT and SGK636-SO (authentic standards) were performed by an Agilent 1260 Infinity II LC-MS chromatographic system comprised of a G7115A 1260DAD WR detector, a G7311B 1260 Quad Pump system, a G1328C 1260 Manual Injection unit and a G6125B LC/MSD detector. An ACE C18 column was used as a stationary phase. LC-MS/MS analysis for standards and test extracts were performed in an Agilent 1640 series HPLC system equipped with online degasser, a binary pump, an autosampler, and column oven and interfaced to an Agilent 6460A triple-quadrupole mass spectrometer equipped with an electrospray ionization source (Agilent Technologies, Santa Clara, USA). All raw data were acquired and analyzed using Agilent Masshunter data processing software. A Camag Automatic Developing Chamber (ADC-2) device was used for HP-TLC studies. Densitometric scanning was performed in fluorescence mode using Camag TLC Scanner IV and Vision CATS software after derivation.

Adult male Suffolk white pig was used in this study. ß-Nicotinamide dinucleotide phosphate (disodium salt, NADP) and glucose-6-phosphate (disodium salt, G-6-P) were purchased from Sigma. Glucose-6-phosphate dehydrogenase suspension (Reinheit grade II, 10 mg per 2 ml; G-6-PD) was obtained from Sigma Aldrich. Dichloromethane was obtained from Merck.

Experimental

Synthesis

S-oxide (SGK636-SO) ((*S*)-3-((2,4,6-trimethylphenyl) thioxo)-4-(4-fluorophenyl)-5-(1-(6-methoxynaphtalen-2-yl)ethyl)-4*H*-1,2,4-triazole): To synthesize the authentic *S*-oxide, the substrate (SGK636, 0.001 mol) was dissolved in ethanol (20 ml) and *m*-chloroperoxybenzoic acid (*m*-CPBA, 0.0012 mol) was added dropwise in an ice bath (0-5 °C). The mixture was stirred for 4 hours and the reaction was monitored by TLC. After the reaction completed, ethanol was evaporated under atmospheric pressure and the solid was extracted with dichloromethane/water mixture. The organic phase was evaporated. The solid product was further purified by column chromatography. M.p 168-170°C. FT-IR υmax (cm^{-1}): 3065 (C-H), 1605 (C=N), 1391 (S=O). MS (vAPCI): (M+1) 528.5; 520.6; 353.7; 342.9; 338.3; 327.3. Elemental analysis: $C_{31}H_{30}FN_3O_2S$ Calculated: 67.94 (C%); 5.98 (H%); 6.69 (N%); 5.01 (S%). Found: $C_{31}H_{30}FN_3O_2S$. C_2H_5OH 67.21 (C%); 6.15 (H%); 7.13 (N%); 5.44 (S%). LCMS: (M+1) 528.2

LC-MS Analysis

An acetonitrile (ACN)/water (70/30, v/v) mobile phase mixture was used. The substrate and metabolic standards were separated according to their mass/charge ratio and their molecular ion peaks were determined in the mass spectroscopy section and the retention times (Rt) of the substrate and metabolic standards were recorded. A DAD detector was also used to compare UV spectra of standard and metabolic products.

LC-MS/MS analysis

An acetonitrile (ACN) (100%) mobile phase was used. The substrate and the *S*-oxide metabolic standard were directly applied to triple-quad mass spectrometer. The substrate (SGK 636), *S*-oxide metabolic standard (SGK-636-SO) and incubation extract were analyzed according to their mass/charge ratio. Their molecular ions and fragmentations were recorded.

HP-TLC Analysis

The standard compounds (1mg/ml) were prepared in methanol. Each prepared solution was filtered through a 0.45 µm syringe filter except the incubates. The sample and standard solutions were applied in bands of 8 mm length on silica gel glass HP-TLC plates 60 F_{254} with Camag Automatic TLC Sampler IV. A constant application rate was performed, and the gaps between the tracks were 10 mm. The mobile phase was petroleum ether/dichlorometane/ethyl acetate (25:50:25 v/v/v) at 25°C. The chamber was saturated for 20 min, and the plate was pre-conditioned for 5 min before the development. The humidity is controlled by ADC-2 using $MgCl_2$ (33% RH) for 10 minutes. Densitometric scanning was performed in fluorescence mode using Camag TLC Scanner IV and Vision CATS software after derivation. The slit size was kept at 5×0.2 mm, the micro and scan speeds were set at 20 mm/s.

Biological Studies

The animals were deprived of food overnight prior to sacrifice, but were allowed water ad libitum. They were previously fed on a balanced diet. Hepatic washed pig microsomes were prepared as described by Schenkman and Cinti (37) and Ulgen (38).

Incubation and Extraction Procedures

Incubations were carried out in a shaking water bath at 37°C using a standard co-factor solution consisting of NADP (2 µmole), G-6-P (10 µmole), G-6-PD suspension (1 unit) and aqueous $MgCl_2$ (50% w/w) (20 µmole) in phosphate buffer (0.2M, pH 7.4, 2 ml) at pH 7.4. Co-factors were pre-incubated for 5 min to generate NADPH, before the addition of microsomes (1 ml equivalent to 0.5 g original liver) and substrate (5 µmole) in methanol (50 µl). Briefly, seven test tubes were prepared (3 for test, 4 for controls) and co-factors (2ml in each tube), microsomal fraction (1 ml for each tube) and substrate (50 µl for each tube) were added respectively. The incubation was continued for 30 min, terminated and extracted with dichloromethane (3x5 ml). The organic extracts were evaporated to dryness under a steream of nitrogen (3).The residues were reconstituted in methanol (200 µl) for LC-MS and LC-MS/MS. The reconstituted extracts were analysed using the reverse-phase LC-MS system described in the text. Test extracts were further investigated in LC/MSMS. For HPTLC studies, these samples (dissolved in 50 µl metanol per sample) were also analysed using HPTLC equipment.

Autooxidation Studies

Either the substrate (2 µM) (SGK636) or authentic *S*-oxide standard (SGK636-SO) (2 µM) was dissolved in methanol (50 µl). Then, phosphate buffer (0.2 M, pH 7.4) (3ml) was added in the same incubation conditions as test experiments. The incubation was continued for 30 min, terminated and extracted with dichloromethane (3x5 ml). The organic extracts were evaporated to dryness under a steream of nitrogen (3).The residues were reconstituted in methanol (200 µl) for LC-MS and LC-MS/MS. The reconstituted extracts were analyzed using the reverse-phase LC-MS system described in the text. Test extracts were further investigated in LC-MS/MS. For HP-TLC studies, these samples (dissolved in 50 µl methanol per sample) were also analyzed using HP-TLC equipment.

Denaturation of Microsomes

For control experiments, microsomes were denaturated using boiling water. The necessary amount of freshly defrosted microsomes were taken in a test tube and it was placed in boiling water for 5 mins. After the heat-denaturation, the denatureated microsomes were used for control experiments.

***In Silico* Studies**

Our study group aimed to observe how the compound binds to P450 CYP3A4 protein, which probably causes its *S*-oxidation, using *in silico* approaches in the light of experimentally obtained information. For this purpose, the X-RAY crystal structure of the protein (PDB ID: 4D7D) was retrieved from the Protein Data Bank server (www.pdb.org, accessed 08 September 2022). Schrödinger Maestro Schrödinger Release 2020-3, Maestro, Schrödinger, LLC, New York, NY, USA (2020) interface was used for the molecular docking study and the enzymes crystals were processed using the Protein Preparation Wizard protocol of the Schrödinger Suite 2020. Compounds were prepared using the LigPrep module Schrödinger Release. 2020-1: LigPrep 2020, Schrödinger, LLC, New York, NY, USA (2020) to correctly assign the protonation states (pH=7.4) as well as the atom types. Bond orders were assigned, and hydrogen atoms were added to the structures. The grid generation was formed using the Glide module Schrödinger Release 2020-3, Glide, Schrödinger, LLC, New York, NY, USA (2020), and docking runs were performed in standard precision docking mode (SP).

After determining the best pose for ligand-enzyme complex, we aimed to determine and clarify the changes in the interactions during the time and environmental changes using molecular dynamic simulation (MDS) technics. Thus, an MDS study was performed for 100 ns with the POPE transmembrane model system and 3 points (TIP3P) water model followed by energy minimization of the complex waters. The neutralization of the system was achieved using Na^+ and Cl^- ions and 150 mM NaCl was added. The molecular dynamic simulation was performed following the completion of the system setup. The radius of gyration (Rg), root mean square fluctuation (RMSF), and root mean square deviation (RMSD) values were calculated by the Desmond application Schrödinger Release 2020, Desmond, Schrödinger, LLC, New York, NY, USA (2020) and perused to previous literatures (39-40).

RESULTS AND DISCUSSION

The aim of this present study is first to observe and prove any qualitative *in vitro* microsomal metabolite formation of the anticancer drug candidate, SGK636. The formation of the metabolites was proved in LC-MS, LC-MS/MS and HP-TLC analyses. There are limited data available on HP-TLC and microsomal metabolism studies in the literature. This study is the first representative on this field in terms of HP-TLC usage in in vitro microsomal metabolism studies (41).

LC-MS, LC-MS/MS and HP-TLC

Several attempts were made in order to separate SGK636, DT and the corresponding *S*-oxide (SGK636-SO) with LC-MS and HPTLC. Acetonitrile/water (70:30, v/v) was found to be the best mobile phase for the LC-MS separation of substrate and its metabolites (Figure 1a) and the best mobile phase for HP-TLC was a mixture of petroleum ether (40-60°C)/dichloromethane/ethyl acetate (25:50:25 v/v/v) at 25 °C (Figure 4). The retention times and Rfx100 values of the compounds were recorded (Table 1).

Table 1 Chromatographic properties of the substrate and the potential metabolites (**SGK636, DT** and **SGK636-SO**).

Compound (abbreviation)	M.W. (g/mol)	Molecular ion peak (M+1) (m/z)	HPTLC Rfx100 values	LC-MS retention time (min)
Substrate (**SGK636**)	512.20	513	35.8	15.05
Dealkylated thiole (**DT**)	379.11	380	74.7	4.68
SGK636 S-oxide (**SGK636-SO**)	527.20	528	16.3	7.66
for HPTLC and LC-MS conditions see text				

Following the metabolic experiments using SGK636 as a substrate, no *S*-dealkylation product (DT) was detected by using pig liver microsomes following LC-MS (Figure 1b). After the incubation, the oxidative metabolite (SGK636-SO) was observed with LC-MS (Figure 1b) analyses. The control experiments with denaturated microsomes or in the absence of co-factors were also carried out to establish whether the *S*-oxidation reaction is enzymatic and co-factor dependent (Figure 1c, 1d). *S*-oxide metabolite was only formed in the presence of enzyme and co-factors but not in the control experiments (in the presence of denaturated microsomes and in the absence of co-factors) indicating that the reaction was enzymatic. In order to establish any autooxidation into the corresponding sulfoxide, the substrate SGK636 was also incubated in buffer under standard incubation conditions (but without enzyme and co-factors) and no autooxidation into the corresponding sulphone was observed. A stability work for SGK636-SO (sulfoxide) in buffer was also performed to see any possible autooxidation to sulphone or reduction back to SGK636. However, no conversion into SGK636 or the corresponding sulphone was observed in either way.

The authentic and metabolically formed SGK636-SO were compared with their retention times, UV and MS spectra and gave identical Rt and Rfx100 values on LC-MS and HP-TLC and identical spectra in both UV and MS (Figure 1, 2, 3, 4). LC-MS/MS analysis also confirmed the formation of sulfoxide (*S*-oxide metabolite). The fragmentations were recorded as their *m/z* values. Both substrate (SGK 636) and *S*-oxide metabolic standard (SGK 636-SO) were found to be stable in terms of fragmentation (Figure 5, 6, 7).

Further study was performed for the incubation of *S*-oxide metabolic standard compound, SGK636-SO. The result presented that the corresponding sulfoxide is further oxidized to sulfone derivative. The sulfone formation was proved in LC-MS analysis (Figures 8a and 8b).

The experiments were performed with test and control incubation systems. We have also included the autooxidation procedure for both substrate and the authentic metabolic standards (Figure 9). The control incubation procedures consisted of 'denaturated microsomes'. The denaturation of the microsomes was provided by placing the mixture into hot boiling bath for 5 mins. The 'heat inactivation' procedure was performed for providing denaturated microsomes. Although this study does not cover the enzymatic profile, some critical assumptions can be made in terms of enzymatic pathways. Sulphur oxidation is mainly provided by FMO enzymes rather than CYP enzymes. A few studies indicates the oxidation mechanism of sulphur containing molecules regarding biotransformation. A study showed the enzymatic participation of P450 and FMO in fenthion biotransformation. When recombinant P450s are used, CYP2C19 was found to be responsible for sulfoxide formation. CYP1A1, CYP3A4 and CYP3A7 was also found to have a significant role in sulfoxide formation (42). When human liver microsomes used at low concentration of fenthion, sulfoxidation is predominantly P450-mediated. At the high concentrations, FMO's get on the line (43). Rawden and co-workers studied the metabolic sulfoxidation profile of albendazole using human liver microsomes. *In vivo* studies mostly hold CYP enzymes responsible for sulfoxide formation. Recombinant CYP3A4, CYP1A2 and FMO3 produced more sulfoxide of albendazole than control microsomes. This study presented that the formation of sulfoxide depends on CYP activation, rather than FMO; primarily CYP3A4 was found to be most relatively involved in oxidation reaction (44). In our study male pig liver microsomes were used as consistent with the literature (45). Using this literature data, it may be assumed that the formation of sulfoxide mostly depends on CYP activation, as there was no metabolite formed in control experiments.

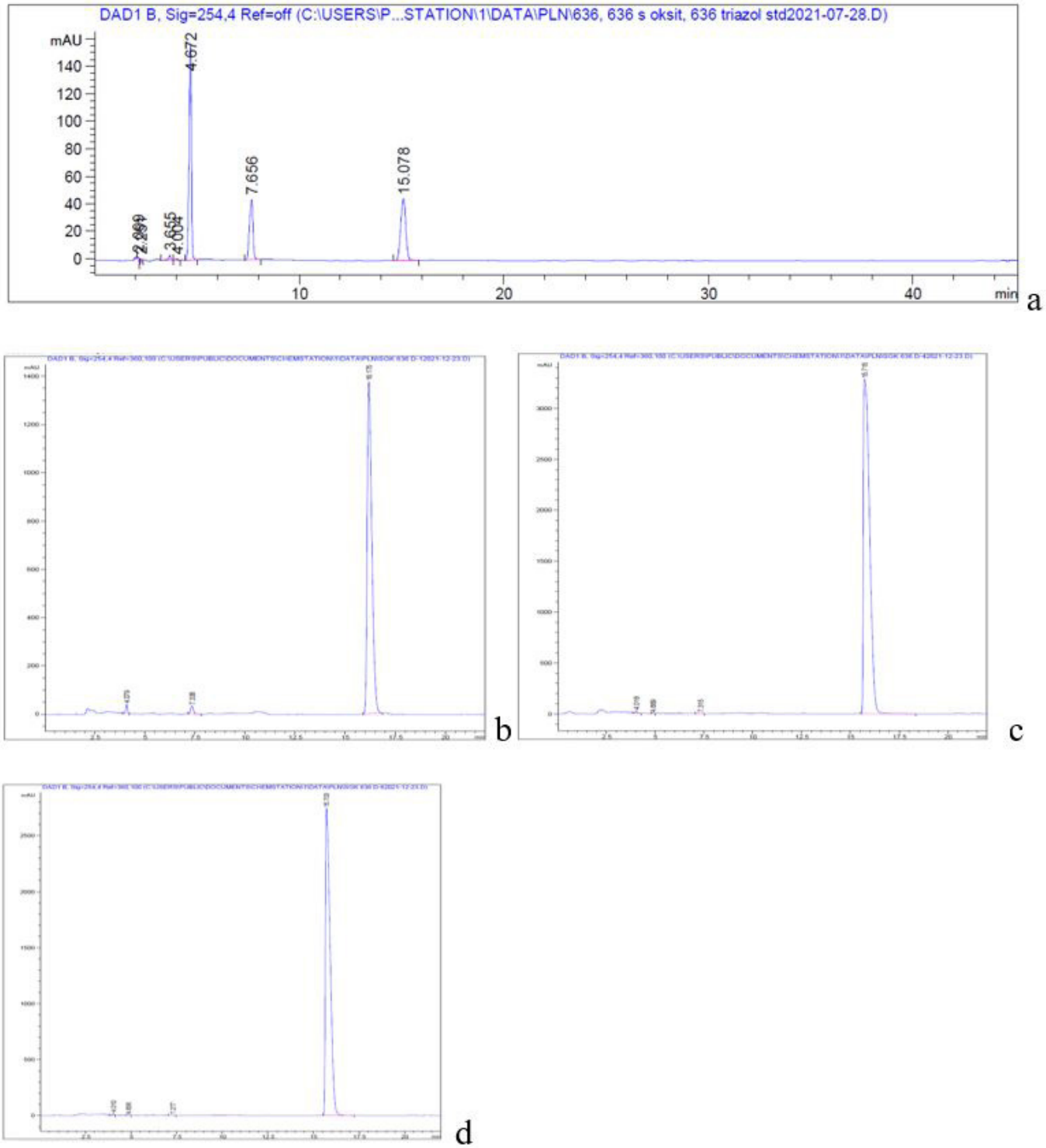

Figure 1. *(a), HPLC chromatogram of substrate (SGK636: 15.078) and its metabolic standarts (DT: 4.672 and SGK636-SO: 7.656) (b), HPLC chromatogram from SGK636 test mixture (c) HPLC chromatogram from SGK636 control experiment without microsomes (d) HPLC chromatogram from SGK636 control experiment without co-factors (see Table 1 for abbreviations)*

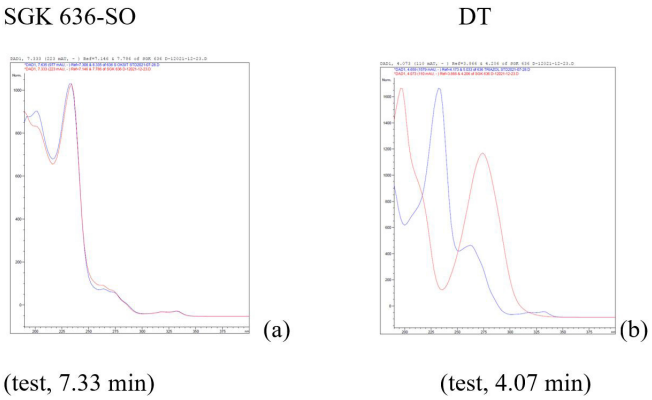

Figure 2. *(a) UV spectrum of standard and metabolic SGK636-SO; (b) standard DT and metabolically formed unknown metabolite (see text for abbreviations) (note: although the retention times were the same (4.07 min), their UV spectra were different indicating the metabolite is different from DT)*

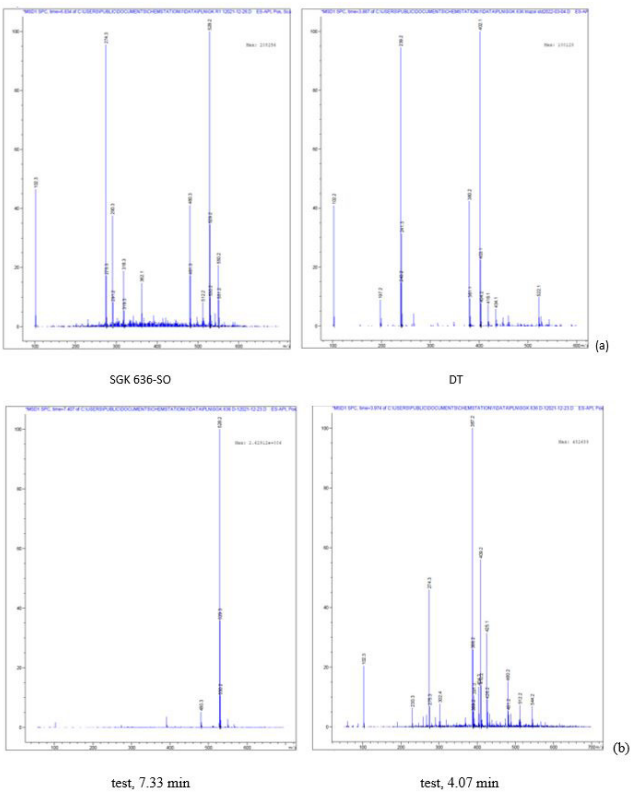

Figure 3. *(a) Mass spectrum of standard SGK636-SO and DT (b) Mass spectrum of SGK636-SO metabolite and unknown metabolite from SGK636 test mixture following incubation of SGK636 with pig liver microsomes fortified with NADPH*

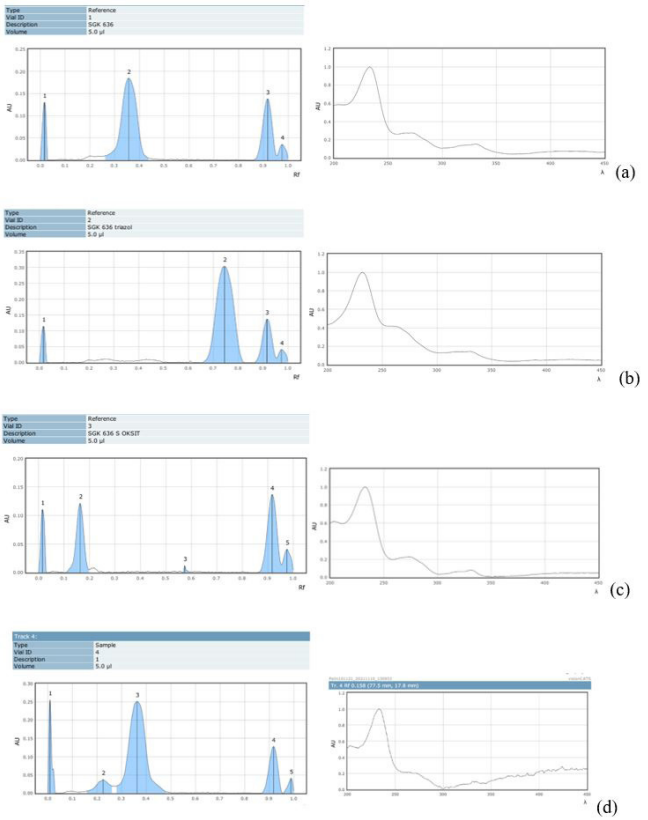

Figure 4. *HPTLC chromatogram and UV spectra of (a) SGK636, (b) DT, (c) SGK636-SO (peak 2: standard compounds, i.e. peak 2 for a is SGK636; peak 2 for b is DT; peak 2 for c is SGK636-SO. All other peaks are related to solvents used) and (d) in-vitro metabolic extract from SGK636 metabolism with pig liver microsomes fortified with NADPH (peak 2 for d is SGK636-SO; peak 3 for d is SGK636, all other peaks are related to solvents used) (see Table 1 for specific Rfx100 values).*

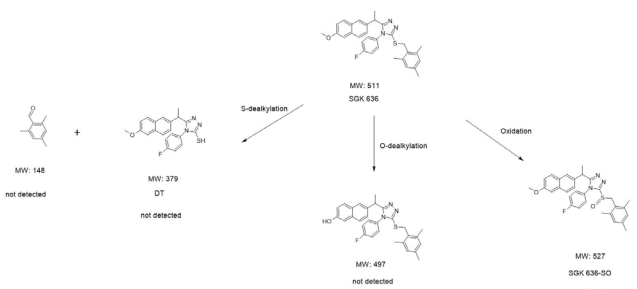

Figure 5. *Metabolic profile of **SGK636** and molecular weights of metabolites (see text for abbreviations)*

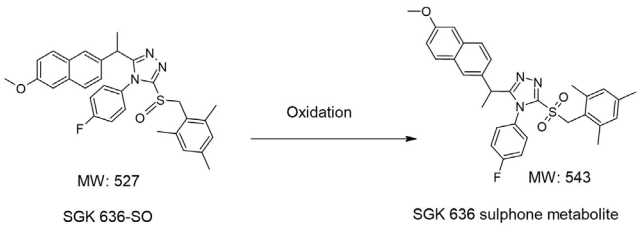

Figure 6. *S-oxidation profile of SGK 636-SO*

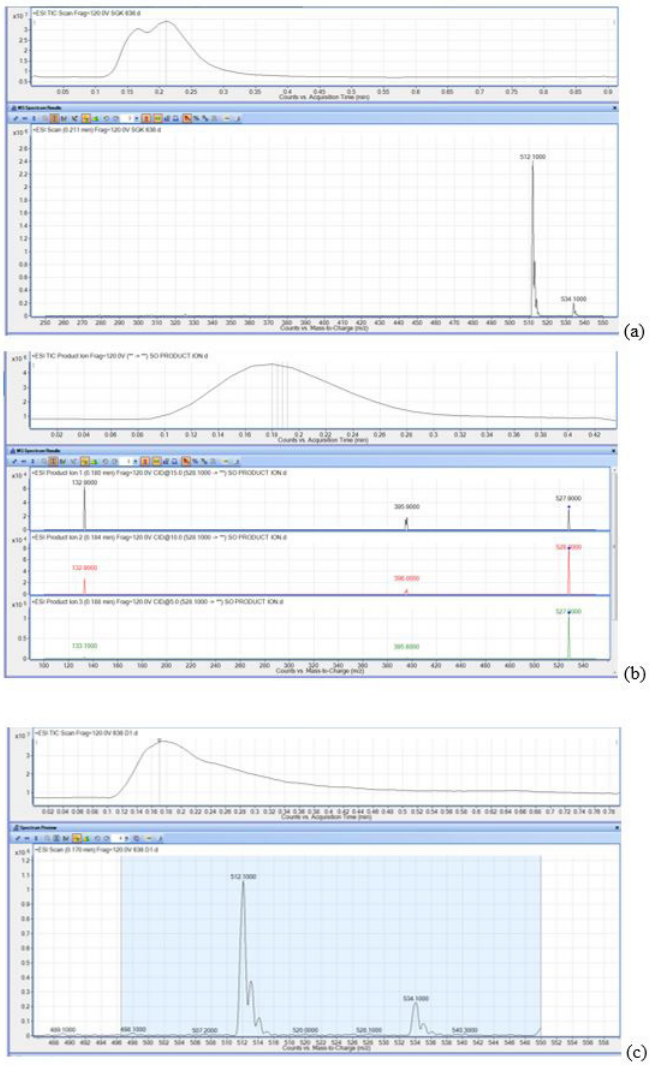

Figure 7. *LC-MS/MS results for SGK636, authentic S-oxide standard and test experiment: (a) LC-MS/MS analysis of standard substrate (SGK 636) (b) LC-MS/MS analysis of SGK 636-SO standard (c) SGK 636 Test (512 is substrate and 528 is S-oxide metabolite)*

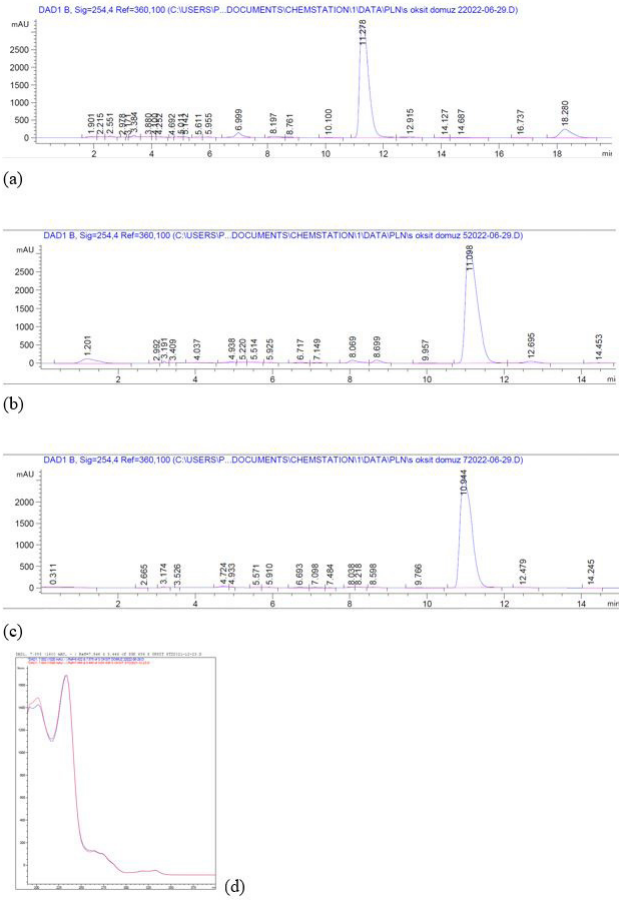

Figure 8a. *Authooxidation of SGK636 and SGK636-SO; (a) HPLC chromatogram of SGK 636-SO test incubation (b) HPLC chromatogram of SGK 636-SO control (with no microsomes) (c) HPLC chromatogram of SGK 636-SO control (with no co-factor) (d) UV comparison of SGK 636-SO and sulfone metabolite*

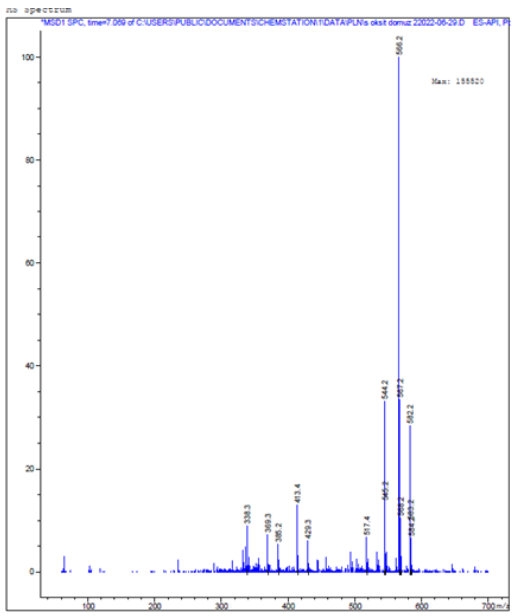

Figure 8b. *Authooxidation of SGK636 and SGK636-SO; Mass spectrum of SGK 636-SO sulphone metabolite in 6.99 min (544 resulted from sulfone metabolite)*

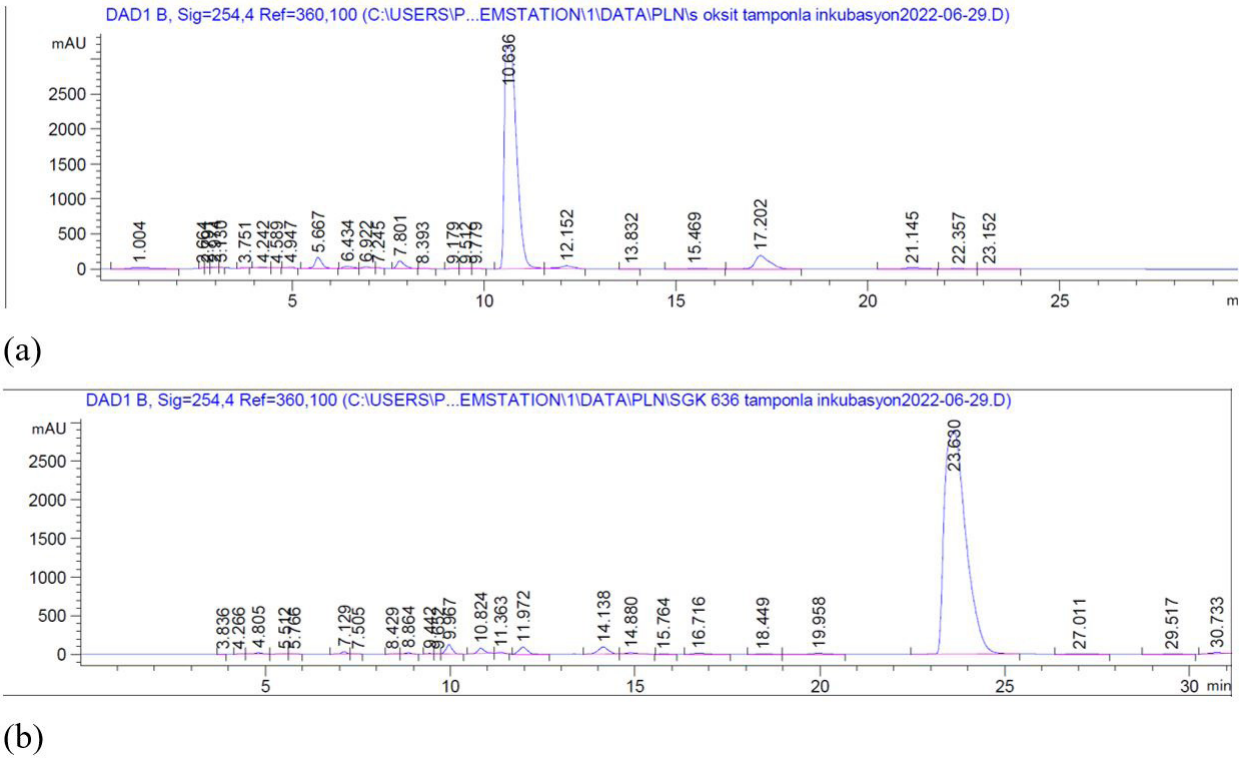

Figure 9. *Autooxidation study of SGK636 and SGK636-SO standard; (a) HPLC chromatogram of SGK 636-SO incubation with buffer (b) HPLC chromatogram of SGK636 incubation with buffer*

An unknown metabolite was also observed only in the test tubes at 4.07 min (Figure 1b). That peak could not belong to the *S*-dealkylated metabolite (DT) since its UV and MS spectrum were not identical with the authentic standard (Figure 2 and 3). It can not be O-dealkylation metabolite either (Figure 2 and 3) as this unknown product has a different molecular weight (MW: 387) compared to the calculated value for *O*-dealkylation metabolite (MW: 497) (Figure 5).

HP-TLC results also indicated the formation of SGK636-SO (Figure 4) (see Table 1 for Rfx100 values). The existence of this sulfoxide metabolite was confirmed by the identical Rfx100 values and UV spectra of authentic and metabolically formed SGK636-SO (Figure 4).

According to the previous study (46), the possible biotransformation site (SOM) of the ligands in the ligand-CYP3A4 enzyme complex can be determined if it is within 6.0 Å from the iron atom of heme. In fact, the methodology behind the determination of possible SOMs is applicated using the extra-precision (XP) or induced-fit (IF) docking methods because the CYP3A4 is very flexible enzyme.

But in this case, since we have a known metabolite obtained from experimental study and thus not searching for possible metabolites, we used the standard precision (SP) docking method. The docking result (Figure 10) revealed that SGK636 ligated to the substrate region of the enzyme and contacted the iron atom of the HEM protein. This was observed as π-cation interaction. Also, there was an aromatic H-bond between H3 of 4-fluorophenyl and Ser119 amino acid. These two interactions pointed out that the ligand and the complex adapted to each other, thus, it is also suggested that one of the possible biotransformation mechanisms is probably catalyzed by Cyp3A4. Additionally, Ser119 amino acid is described as a key residue to stabilize the complex (47).

According to the docking study, there were three possible sites on SGK636 to oxidate, one is a sulfur atom, one is methyl group of 2,4,6-trimethylphenyl and the other one is a methyl group of ethyl bridge. To clarify this issue and understand the binding mode versus conformational changes by time-dependent and environmental changes, we also performed a molecular dynamics simulation study. The MDS data was shared in Figure 11.

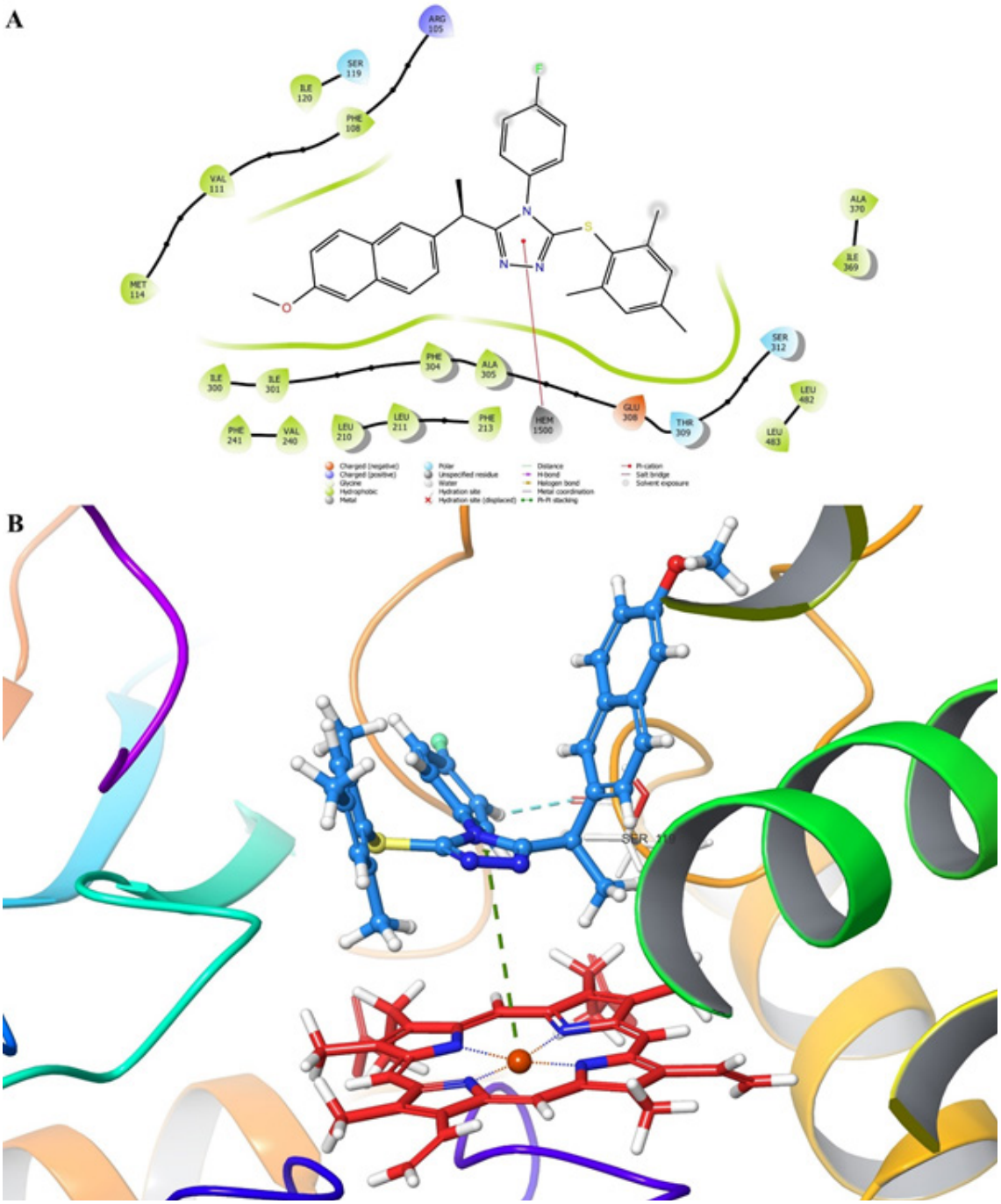

Figure 10. *2D (**A**) and 3D (**B**) representations of the compound at Cyp3A4 substrate pocket (PDBID: 4D7D). The Green dashed lines are used for π-cation and the cyan dashed lines are used for the aromatic hydrogen bond.*

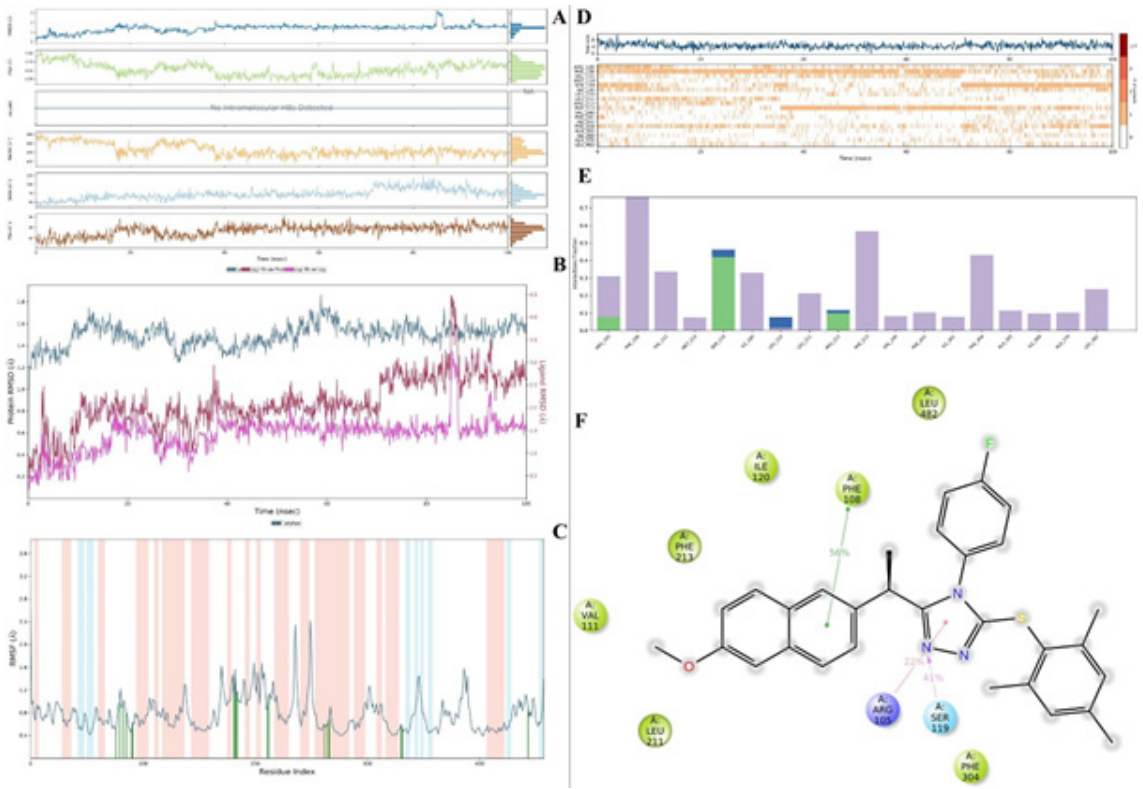

Figure 11. *MDS results for the compound and CYP3A4 protein complex.* ***A-C:*** *The stability properties of the complex.* ***A:*** *Physicochemical properties of the ligand;* ***B:*** *RMSD plot of the protein, the ligand versus protein and the ligand versus ligand;* ***C:*** *RMSF plot of the complex.* ***D-E:*** *The contacts properties of the complex.* ***D:*** *Number of interactions and interaction types versus time plot;* ***E:*** *Plot of interaction fractions versus residues with their interaction types during the time;* ***F:*** *2D diagram for contact strength (cutoff = 20%).*

The stability criteria (48-49) were found in acceptable ranges. Rg values decreased around 0.5 Å from 0 to 36.60 ns, after that, their changes were observed between 0.25 Å. RMSD values of protein were observed between 1.00-1.86 Å (RMSDmax was observed at 58.80 ns). RMSD values of ligand were observed between 0.36-3.26 Å and 0.92-4.48 Å, according to itself and the protein, respectively. And the RMSF values were observed as expected, for the rigid structures (helixes and strands), they were observed under 1.2 Å, and if there was a contact, then these values were under 0.8 Å. Besides that, the RMSF values of interacted flexible structures (loops) were observed under 1.2 Å. Specifically, the RMSF value of Ser119 was determined as 0.54 Å. As a result, all these criteria guaranteed that the MDS results are reliable. So, the interactions and their properties could be evaluated to understand the behavior of the complex. Direct H-bonds were observed with Arg105, Ser119, and Arg212 amino acids. Aromatic H-bonds formed with Ser119, Leu210, Arg212, Phe241, Ala370, and HEM1500 residues, and water-mediated H-bonds were with Ser119, Leu210 and Arg212 amino acids. The hydrophobic interactions were with Arg105, Phe108, Val111, Met114, Ile120, Leu211, Phe213, Val240, Phe241, Ile301, Phe304, Ala305, Ile369, Ala370, and Leu482 amino acids. Furthermore, especially, the interactions with Phe118, Ser119, and Arg105 had a pivotal role in ligating to CYP3A4 enzyme by SGK636, were noted.

The histograms of the distance values frequency were shared in Figure 12 (AH and BH). Also, in MDS video, the purple dashed line and its number represent the distance between the iron of Hem and the sulfur atom or methyl group of SGK636. The distance changes during the time (ps) were also plotted in Figure 12 (AP and BP). As seen, while the methyl group of 2,4,6-trimethylphenyl digressed from HEM, the sulfur atom was getting closer to iron of HEM. Therefore, it's clearly said that this methyl group is not a favorable candidate for SOM. Moreover, as seen in the MDS video, the methyl group of ethyl localized outside to do not contact with the HEM (>10 Å). As mentioned, if the maximal distance between SOM and iron of HEM is 6 Å, the CYP enzymes can catalyze the xenobiotic. In this MDS study, the mean value (distance between iron and S atom) was calculated as 5.248±0826 Å during the entire simulation. (As the mean value (for between iron and CH3 of the 2,4,6-trimethylphenyl group) was meaningless, it was not calculated).

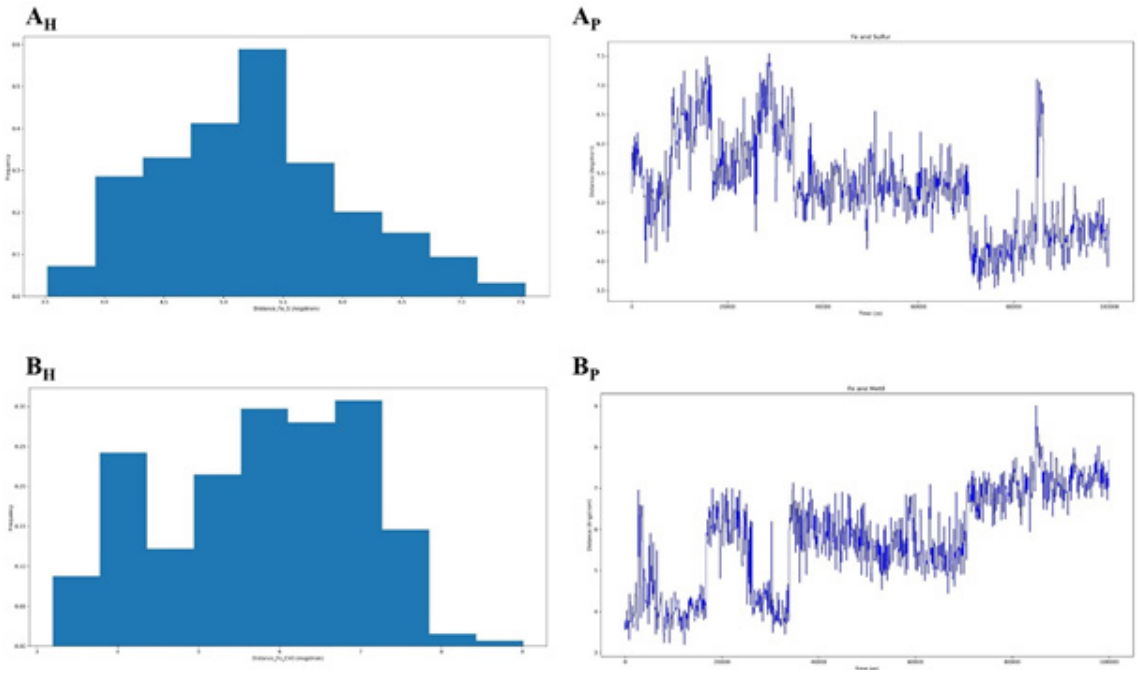

Figure 12. *The fractions of the distances between the iron of HEME and (**A**) sulfur atom or (**B**) methyl group.* $_H$ *for histogram of frequency versus distances,* $_P$ *for plot of distance versus time.*

As a result, this MDS study revealed that there is only one possibility, and this possible SOM of SGK636 is upon *S*-oxidation. Since our experimental study also proved the obtained metabolite was *S*-oxide-SGK636, *in vitro* and *in silico* studies are in harmony.

CONCLUSION

The present metabolic study indicates that an anticancer drug candidate, SGK 636 converted to the corresponding *S*-oxide metabolite following its *in vitro* microsomal metabolism by pig liver microsomes but no any dealkylated metabolite was observed. The *in silico* studies also proved the *S*-oxidation via CYP3A4 enzyme. Since sulfoxidation process can be reversible and it may partly explain the low amount of sulfoxide metabolite, SGK636-SO (sulfoxide) was also incubated but no metabolic or chemical conversion into the SGK636 was observed. However, it produced the corresponding sulfone metabolite. This was established by LC-MS. The findings also indicate that this substrate is very stable to metabolic *S*- or *O*-dealkylation reactions which could be an advantage in terms of its pharmacological activity. The *S*-oxide metabolite was detected and confirmed by comparison with retention times, Rfx100 values, UV and MS spectra of authentic and metabolic product using LC-MS, LC-MS/MS and HP-TLC techniques. Further study was performed for the incubation of *S*-oxide metabolic standard compound, SGK636-SO. The result presented that the corresponding sulfoxide is further oxidized to sulfone derivative. The sulfone formation was proved in LC-MS analysis. An unknown product was also observed following metabolic experiment which did not correspond to the molecular weight of any dealkylation metabolite or of any possible metabolic conversion product. In order to establish if the *S*-oxidation reaction is enzymatic and/or requires co-factors, control experiments were carried out using denaturated microsomes, buffer instead of co-factors. In additon, the substrate was also incubated with buffer under standard incubation conditions (but without any enzyme and/or co-factors) to find out any autooxidation into corresponding sulfoxide and no autooxidation was observed.

Acknowledgement

The synthesis and confirmation SGK636 and (S)-Naproxen triazole were supported by a grant of TUBITAK (Project number: 215S009). (+) (S)-Naproxen, was obtained from Deva Ilaç San. Tic. A. S. , Turkey. The pig livers were donated by Acibadem University, Animal Laboratory Centre from the Project by Dr. Mehmet Emin Aksoy; laparoscopic and robotic surgery course, with the 2021-01 ethical approval number. The liver tissue was obtained from the euthanized pig at the end of course. Authors are gratefull to Chemist Ummet Melikoğlu (Acıbadem LABMED

employee) for performing LC-MS/MS analyses for the compounds.

Ethics Approval And Consent To Participate

The pig livers were donated by Acibadem University, Animal Laboratory Centre from the Project by Dr. Mehmet Emin Aksoy; laparoscopic and robotic surgery, with the 2021-01 ethical approval number. At the end of the training, liver tissue was obtained from the euthanized pig.

Human And Animal Rights

No humans were used in this study. All animal research procedures were followed in accordance with the standards set forth in the eighth edition of Guide for the Care and Use of Laboratory Animals (published by the National Academy of Sciences, The National Academies Press, Washington, D.C.).

Conflict of Interest

The authors declare no conflicts of interest, financial or otherwise.

REFERENCES

1. Jokanovic´, M. Biotransformation of organophosphorus compounds. Toxicology 2001, 166, 139–160. https://doi.org/10.1016/s0300-483x(01)00463-2
2. Damani, L. A., Thioethers, thiols, dithioic acids and disulphides: Phase I reactions In Sulphur-Containing Drugs and related Organic Compounds. Chemistry, Biochemistry and Toxicology, Damani, L. A., Ed. Ellis Horwood Limited: 1989; Vol. 1, pp 131-146. (Doi number is not applicable)
3. Ziegler, D. M., S-Oxygenases, I: Chemistry and Biochemistry In Sulphur-Containing Drugs and related Organic Compounds. Chemistry, Biochemistry and Toxicology. Part A, Ellis Horwood Limited: 1989; Vol. 2, pp 53-66. Doi number is not applicable)
4. Mitchard, R. L. M. a. J. A. B., H2 receptor antagonists. In Sulphur-Containing Drugs and related Organic Compounds. Chemistry, Biochemistry and Toxicology, 1989, pp 54-87. (Doi number is not applicable)
5. Rydberg, P., Ryde, U., Olsen, L., Sulfoxide, Sulfur, and Nitrogen Oxidation and Dealkylation by Cytochrome P450. J Chem Theory Comput 2008, 4 (8), 1369-77. https://doi.org/ 10.1021/ct800101v
6. Xie, G., Cheng, K. W., Huang, L., Rigas, B., The in vitro metabolism of phospho-sulindac amide, a novel potential anticancer agent. Biochem Pharmacol 2014, 91 (2), 249-55. https://doi.org/ 10.1016/j.bcp.2014.07.007
7. Gurpinar, E., Grizzle, W. E., Piazza, G. A., COX-Independent Mechanisms of Cancer Chemoprevention by Anti-Inflammatory Drugs. Front Oncol 2013, 3, 181. https://doi.org/ 10.3389/fonc.2013.00181
8. Li, C., Zhang, L., Zhang, C., Hirao, H., Wu, W., Shaik, S. Which Oxidant Is Really Responsible for Sulfur Oxidation by Cytochrome P450?. Angew. Chem. Int. Ed. 2007, 46, 8168–8170. https://doi.org/ 10.1002/anie.200702867
9. DuBois, R. N.; Giardiello, F. M.; Smalley, W. E., Nonsteroidal anti-inflammatory drugs, eicosanoids, and colorectal cancer prevention. Gastroenterol Clin North Am 1996, 25 (4), 773-91. https://doi.org/10.1016/s0889-8553(05)70274-0
10. Srinivas, S.; Feldman, D., A phase II trial of calcitriol and naproxen in recurrent prostate cancer. Anticancer Res 2009, 29 (9), 3605-10. PMID: 19667155
11. Lubet, R. A.; Steele, V. E.; Juliana, M. M.; Grubbs, C. J., Screening agents for preventive efficacy in a bladder cancer model: study design, end points, and gefitinib and naproxen efficacy. J Urol 2010, 183 (4), 1598-603. https://doi.org/ 10.1016/j.juro.2009.12.001
12. Kim, M. S.; Kim, J. E.; Lim, D. Y.; Huang, Z.; Chen, H.; Langfald, A.; Lubet, R. A.; Grubbs, C. J.; Dong, Z.; Bode, A. M., Naproxen induces cell-cycle arrest and apoptosis in human urinary bladder cancer cell lines and chemically induced cancers by targeting PI3K. Cancer Prev Res (Phila) 2014, 7 (2), 236-45. https://doi.org/ 10.1158/1940-6207.CAPR-13-0288
13. Han, M. I.; Kucukguzel, S. G., Anticancer and Antimicrobial Activities of Naproxen and Naproxen Derivatives. Mini Rev Med Chem 2020, 20 (13), 1300-1310. https://doi.org/ 10.2174/1389557520666200505124922
14. Han, M. İ. B., H. ; Cumaoğlu, A.; Küçükgüzel, Ş. G. , Synthesis and characterization of 1,2,4-triazole containing hydrazide-hydrazones derived from (S)-Naproxen as anticancer agents. Marmara Pharm. J (now J. Res. Pharm.), 2015, 22 (4), 559-569. https://doi.org/ 10.12991/jrp.2018.98
15. Han, M. I.; Bekci, H.; Uba, A. I.; Yildirim, Y.; Karasulu, E.; Cumaoglu, A.; Karasulu, H. Y.; Yelekci, K.; Yilmaz, O.; Kucukguzel, S. G., Synthesis, molecular modeling, in vivo study, and anticancer activity of 1,2,4-triazole containing hydrazide-hydrazones derived from (S)-naproxen. Arch Pharm (Weinheim) 2019, 352 (6), e1800365. https://doi.org/ 10.1002/ardp.201800365
16. Birgul, K.; Yildirim, Y.; Karasulu, H. Y.; Karasulu, E.; Uba, A. I.; Yelekci, K.; Bekci, H.; Cumaoglu, A.; Kabasakal, L.; Yilmaz, O.; Kucukguzel, S. G., Synthesis, molecular modeling, in vivo study and anticancer activity against prostate cancer of (+) (S)-naproxen derivatives. Eur J Med Chem 2020, 208, 112841. https://doi.org/ 10.1016/j.ejmech.2020.112841
17. Han, M. I.; Atalay, P.; Tunc, C. U.; Unal, G.; Dayan, S.; Aydin, O.; Kucukguzel, S. G., Design and synthesis of novel (S)-Naproxen hydrazide-hydrazones as potent VEGFR-2 inhibitors and their evaluation in vitro/in vivo breast cancer models. Bioorg Med Chem 2021, 37, 116097. https://doi.org/ 10.1016/j.bmc.2021.116097
18. Birgül, K. U., A.I.; Çuhadar, O.;, Koçyiğit, S.; Tiryaki, S.; Mega, T.P.; Orun, O.;, Telci, D.; Yılmaz, Ö.; Yelekçi, K.; Küçükgüzel, Ş.G. , Synthesis and Molecular Modeling of MetAP2 of Thiosemicarbazides, 1,2,4-triazoles, thioethers derived from (S)-Naproxen as Possible Breast Cancer Agents. Journal of Molecular Structure 2022, 132739. https://doi.org/ 10.1016/j.molstruc.2022.132739
19. Han, M. İ., Tunç, C.Ü. Atalay,, P.; Erdoğan, Ö.; Ünal, G.; Bozkurt, M.; Aydın, Ö.; Çevik, Ö.; Küçükgüzel, Ş.G. . , Synthesis, characterization, in vitro and in vivo anticancer activity studies of new (S)-Naproxen thiosemicarbazide/1,2,4-triazole derivatives. New J. Chemistry 2022, in press. https://doi.org/ 10.1039/D1NJ05899A
20. Deb, J.; Majumder, J.; Bhattacharyya, S.; Jana, S. S., A novel naproxen derivative capable of displaying anti-cancer and anti-migratory properties against human breast cancer cells. BMC Cancer 2014, 14, 567. https://doi.org/ 10.1186/1471-2407-14-567
21. Kucukguzel, I.; Kucukguzel, S. G.; Rollas, S.; Kiraz, M., Some 3-thioxo/alkylthio-1,2,4-triazoles with a substituted thiourea moiety as possible antimycobacterials. Bioorg Med Chem Lett 2001, 11 (13), 1703-7. https://doi.org/ 10.1016/s0960-894x(01)00283-9

23. Kucukguzel, S. G.; Kucukguzel, I.; Tatar, E.; Rollas, S.; Sahin, F.; Gulluce, M.; De Clercq, E.; Kabasakal, L., Synthesis of some novel heterocyclic compounds derived from diflunisal hydrazide as potential anti-infective and anti-inflammatory agents. Eur J Med Chem 2007, 42 (7), 893-901. https://doi.org/ 10.1016/j.ejmech.2006.12.038

24. Kucukguzel, I.; Tatar, E.; Kucukguzel, S. G.; Rollas, S.; De Clercq, E., Synthesis of some novel thiourea derivatives obtained from 5-((4-aminophenoxy)methyl)-4-alkyl/aryl-2,4-dihydro-3H-1,2,4-triazole-3-thiones and evaluation as antiviral/anti-HIV and anti-tuberculosis agents. Eur J Med Chem 2008, 43 (2), 381-92. https://doi.org/ 10.1016/j.ejmech.2007.04.010

25. Kucukguzel, S. G.; Cikla-Suzgun, P., Recent advances bioactive 1,2,4-triazole-3-thiones. Eur J Med Chem 2015, 97, 830-70. https://doi.org/ 10.1016/j.ejmech.2014.11.033

26. Cikla-Suzgun, P.; Kaushik-Basu, N.; Basu, A.; Arora, P.; Talele, T. T.; Durmaz, I.; Cetin-Atalay, R.; Kucukguzel, S. G., Anti-cancer and anti-hepatitis C virus NS5B polymerase activity of etodolac 1,2,4-triazoles. J Enzyme Inhib Med Chem 2015, 30 (5), 778-85. https://doi.org/ 10.3109/14756366.2014.971780

27. Coşkun, G. P. Djikic., T.; Hayal, T.B.; Türkel, N.; Yelekçi, K.; Şahin, F.; Küçükgüzel, Ş. G. , Synthesis, Molecular Docking and Anticancer Activity of Diflunisal Derivatives as Cyclooxygenase Enzyme Inhibitors. Molecules 2018, 23, 1969. https://doi.org/ 10.3390/molecules23081969

28. Coşkun, G. P. D., T.; Kalaycı, S.; Yelekçi, K.; Şahin, F.; Küçükgüzel, Ş.G. , Synthesis, Molecular Modelling and antibacterial activity against Helicobacter pylori of novel diflunisal derivatives as urease enzyme inhibitors. Letters in Drug Design and Discovery 2019, 16 (4), 392-400. https://doi.org/10.2174/1570180815666180627130208

29. Cikla-Suzgun, P.; Kucukguzel, S. G., Recent Progress on Apoptotic Activity of Triazoles. Curr Drug Targets 2021, 22 (16), 1844-1900. https://doi.org/ 10.2174/1389450122666210208181128

30. Han, M. I.; Ince, U.; Gunduz, M. G.; Kucukguzel, S. G., Synthesis, Antimicrobial Evaluation, and Molecular Modeling Studies of New Thiosemicarbazide-Triazole Hybrid Derivatives of (S)-Naproxen. Chem Biodivers 2022, e202100900. https://doi.org/ 10.1002/cbdv.202100900

31. Coruh, I.; Cevik, O.; Yelekci, K.; Djikic, T.; Kucukguzel, S. G., Synthesis, anticancer activity, and molecular modeling of etodolac-thioether derivatives as potent methionine aminopeptidase (type II) inhibitors. Arch Pharm (Weinheim) 2018, 351 (3-4), e1700195. https://doi.org/ 10.1002/ardp.201700195

32. Yilmaz, O.; Bayer, B.; Bekci, H.; Uba, A. I.; Cumaoglu, A.; Yelekci, K.; Kucukguzel, S. G., Synthesis, Anticancer Activity on Prostate Cancer Cell Lines and Molecular Modeling Studies of Flurbiprofen-Thioether Derivatives as Potential Target of MetAP (Type II). Med Chem 2020, 16 (6), 735-749. https://doi.org/ 10.2174/1573406415666190613162322

33. Han, M. I.; Kucukguzel, S. G., Thioethers: An Overview. Curr Drug Targets 2022, 23 (2), 170-219. https://doi.org/ 10.2174/1389450122666210614121237

34. Kaymakcioglu, B.; Oruc, E.; Ulgen, M.; Rollas, S., The in vitro hepatic microsomal metabolism of 3,5-dimethyl-4-(phenylazo)-(1H)-pyrazole in rats. Drug Metabol Drug Interact 1999, 15 (2-3), 107-14. https://doi.org/ 10.1515/dmdi.1999.15.2-3.107

35. Komurcu, S. G.; Rollas, S.; Ulgen, M.; Gorrod, J. W.; Cevikbas, A., Evaluation of some arylhydrazones of p-aminobenzoic acid hydrazide as antimicrobial agents and their in vitro hepatic microsomal metabolism. Boll Chim Farm 1995, 134 (7), 375-9. PMID: 7546542

36. Kucukguzel, S. G.; Kucukguzel, I.; Ulgen, M., Metabolic and chemical studies on N-(4-chlorobenzyl)-N'-benzoylhydrazine. Farmaco 2000, 55 (9-10), 624-30. https://doi.org/ 10.1016/s0014-827x(00)00077-x

37. Schenkman, J. B.; Cinti, D. L., Preparation of microsomes with calcium. Methods Enzymol 1978, 52, 83-9. https://doi.org/ 10.1016/s0076-6879(78)52008-9

38. Ulgen, M., Techniques in in vitro oxidative microsomal phase I drug metabolism. J.Pharm.Univ.Mar 1993, 9 (2), 165-185. Doi is not available

39. Durmaz, S., Evren, A.E., Saglik, B.N., Yurttas, L., Tay, N.F. Synthesis, anticholinesterase activity, molecular docking, and molecular dynamic simulation studies of 1,3,4-oxadiazole derivatives, Arch Pharm (Weinheim), 2022, e2200294. https://doi.org/10.1002/ardp.202200294

40. Evren, A.E., Nuha, D., Dawbaa, S., Saglik, B.N., Yurttas, L. Synthesis of novel thiazolyl hydrazone derivatives as potent dual monoamine oxidase-aromatase inhibitors, Eur. J. Med. Chem. 2022, 229, 114097. https://doi.org/10.1016/j.ejmech.2021.114097

41. Abdelwahab, N.S., Elshemy, H.A.H. & Farid, N.F. Determination of flutamide and two major metabolites using HPLC–DAD and HPTLC methods. Chemistry Central Journal, 2018, 12, 4. https://doi.org/10.1186/s13065-018-0372-y

42. Leoni, C., Buratti, F.M., Testai, E. The participation of human hepatic P450 isoforms, flavin-containing monooxygenases and aldehyde oxidase in the biotransformation of the insecticide fenthion. Toxicology and Applied Pharmacology, 2008, 233, 343–352. https://doi.org/ 10.1016/j.taap.2008.09.004

43. Rawden, H.C., Kokwaro, G.O., Ward, S.A., Edwards, G. Relative contribution of cytochromes P-450 and favin-containing monoxygenases to the metabolism of albendazole by human liver microsomes. J Clin Pharmacol, 2000, 49, 313-322 https://doi.org/10.1046/j.1365-2125.2000.00170.x

44. Elena Doran, E., Whittington, F.M., Wood, J.D., McGivan, J.D. Characterisation of androstenone metabolism in pig liver microsomes. Chemico-Biological Interactions, 2004, 147, 141–149. https://doi.org/ 10.1016/j.cbi.2003.12.002

45. Matal, J., Tunkova, A., Siller, M., Anzenbacherova, E., Anzenbacher, P. Isolation of two cytochrome P450 forms, CYP2A19 and CYP1A, from pig liver microsomes. J vet.Pharmacol Therap, 2009, 32, 470–476. https://doi.org/10.1111/j.1365-2885.2009.01076.x

46. Lokwani, D.K., Sarkate, A.P., Karnik, K.S., Nikalje, A.P.G., Seijas, J.A. Structure-Based Site of Metabolism (SOM) Prediction of Ligand for CYP3A4 Enzyme: Comparison of Glide XP and Induced Fit Docking (IFD), Molecules, 2020, 25. https://doi.org/10.3390/molecules25071622

47. Kaur, P., Chamberlin, A.R., Poulos, T.L. Sevrioukova, I.F. Structure-Based Inhibitor Design for Evaluation of a CYP3A4 Pharmacophore Model, J Med Chem, 2016, 59, 4210-4220. https://doi.org/10.1021/acs.jmedchem.5b01146

48. Turan, N., Yucel, A.E., Evren, Kandemir, U., Can, O.D. Antidepressant-like effect of tofisopam in mice: A behavioural, molecular docking and MD simulation study, J Psychopharmacol, 2022, 2698811221095528. https://doi.org/10.1177/02698811221095528

49. Nuha, D. Evren, A.E., Kapusiz, Ö., Gül, Ü.D., Gundogdu-Karaburun, N., Karaburun, A.Ç., Berber, H. Design, synthesis, and antimicrobial activity of novel coumarin derivatives: An in-silico and in-vitro study, J Mol Struct, 2022, 134166. https://doi.org/10.1016/j.molstruc.2022.134166